Eur Biophys J (2002) 31: 383–388
DOI 10.1007/s00249-002-0229-z

ARTICLE

Y.-H. Lam · C.J. Morton · F. Separovic

Solid-state NMR conformational studies of a melittin-inhibitor complex

Received: 17 January 2002 / Revised: 21 March 2002 / Accepted: 21 March 2002 / Published online: 22 May 2002

Abstract Melittin is a cytolytic peptide whose biological activity is lost upon binding to a six-residue peptide, Ac-IVIFDC-NH_2, with which it forms a highly insoluble complex. As a result, the structural analysis of the interaction between the two peptides is difficult. Solid-state NMR spectroscopy was used to study the interaction between melittin and the peptide inhibitor. Location of the binding site in the melittin-inhibitor complex was determined using lanthanide ions, which quench NMR resonances from molecular sites that are in close proximity to the unique ion binding site. Our results indicated that the inhibitor binding site in melittin is near Leu13, Leu16 and Ile17, but not near Leu6 or Val8. On the basis of these data we propose that the inhibitor binds to melittin in the vicinity of Ala15 to Trp19 and prevents insertion of melittin into cell membranes by disrupting the helical structure. Supporting evidence for this model was produced by determining the distance, using rotational resonance NMR, between the [1-^{13}C] of Leu13 in melittin and the [3-^{13}C] of Phe4 in the inhibitor.

Keywords Intermolecular distance · Inhibitor · Lanthanide ions · Melittin · Rotational resonance NMR

Introduction

Melittin is an α-helical amphipathic peptide of 26 residues derived from the venom of the honey bee that lyses cell membranes (for a review, see Dempsey 1990). The amino acid sequence of melittin is GIGAVLKVLTTG LPALISWIKRKRQQ-$CONH_2$. Using combinatorial chemistry, a six-residue peptide, Ac-IVIFDC-NH_2, has been found to be an active inhibitor of melittin hemolysis (Blondelle and Houghten 1991; Blondelle et al. 1993). Hydrophobic interactions between the peptide and melittin are suggested as a mechanism of inhibition, preventing melittin interacting with the membrane (Hewish et al. 1996). A number of hexapeptides and a pentapeptide based on the structure of Ac-IVIFDC-NH_2 have been synthesized and their ability to inhibit melittin-induced hemolysis was tested using several spectroscopic techniques (Werkmeister et al. 1993; Rivett et al. 1999). The results of this earlier study indicated that the inhibitors were binding to melittin in the region of the tryptophan residue at position 19 and near the proline region of melittin. The sequence that inhibited melittin hemolysis activity was clarified by activity tests which demonstrated that the tripeptide IFD is essential for inhibition (Rivett et al. 1999).

However, the details of the interaction of melittin and its inhibitor are unknown. Structural studies of a melittin-inhibitor complex can provide not only an understanding of the mechanism of melittin inhibition but also general peptide-peptide interactions. Since the melittin-inhibitor complex is highly insoluble, difficulties arise in structural determination by techniques such as multidimensional solution NMR and X-ray crystallography. The nature of the melittin-inhibitor complex has been studied in our recent work by circular dichroism (CD), solution NMR and solid-state (SS) NMR techniques (Lam et al. 2000), in which we showed that the binding of melittin to inhibitor caused a reduction in the degree of α-helical structure of melittin. An overall structural model of the melittin-inhibitor complex is required before rational selection of site-specific labelled analogues of melittin and the inhibitor can be made for the purpose of intra- and intermolecular distance measurements. In this work, SS-NMR and lanthanide ions were used to ascertain binding sites and determine which points of the peptides to specifically label.

Presented at the Australian Biophysical Society Meeting, 2001

Y.-H. Lam · F. Separovic (✉)
School of Chemistry, University of Melbourne,
Parkville, Victoria 3010, Australia
E-mail: fs@unimelb.edu.au
Tel.: +61-3-83446464
Fax: +61-3-93475180

C.J. Morton
Biota Structural Biology Laboratory,
St. Vincent's Institute for Medical Research,
Melbourne, Victoria 3000, Australia

The location of membrane components relative to the membrane surface has been examined in dimyristoylphosphatidylcholine (DMPC) bilayers using a combination of Dy^{3+} ions and high-resolution ^{13}C CP MAS NMR (for a review, see Henry and Sykes 1994; also Villalain 1996; Gröbner et al. 1999), a method based on site-resolved observation of the nuclear spin-relaxation-enhancement effect. The binding of Dy^{3+} to the bilayer surface permits observation of the quenching of resonances that are in close proximity to the polar interface or at the membrane surface. An indication of the binding sites of the melittin-inhibitor complex was found using Dy^{3+} ions and similar techniques to Gröbner et al. (1999), but in our case the location of melittin is relative to the inhibitor surface rather than the membrane surface. Rotational resonance (RR) NMR (Peersen et al. 1995) techniques were then used to measure intra- and intermolecular distances between labelled sites in the melittin-inhibitor complex.

Materials and methods

Peptide synthesis

The peptides were synthesized by solid phase techniques (Merrifield 1963; Stewart and Young 1984) using Rink amide resin for the inhibitors and TGR resin for melittin. Rink resin and TGR resin (Rink-modified TentaGel) (Stewart and Young 1984; Novabiochem 1999) were purchased from Auspep (Melbourne, Australia) and used without further purification. Details of ^{13}C amino acids and peptide synthesis procedure are given in Lam et al. (2000). The monomeric form of the inhibitor was synthesized using the Fmoc-Cys(acetamidomethyl) (ACM) derivative; since it is stable to trifluoroacetic acid (TFA), ACM is not removed during cleavage. Once the last amino acid was coupled, a final deprotection step was carried out prior to cleavage of the peptide from the resin. In the case of the inhibitor, the N-terminus was acetylated following removal of the terminal Fmoc protecting group. The peptides were characterized by HPLC, mass spectrometry and solution NMR.

Sample preparation

Inhibitor-Dy^{3+}

To inhibitor (40 mg) dissolved in TFA (1 mL), 40 μL of Dy^{3+} in aqueous solution (3.77 mg per 10 mL) was added, mixed and dried under N_2 gas.

Melittin-(inhibitor-Dy^{3+})

Inhibitor with equimolar Dy^{3+} (4.3 mg, ~0.4 mmol) was added to melittin (15 mg, ~0.4 mmol) and both dissolved in TFA (1 mL). Diethyl ether (6 mL) was added and a precipitate formed. Following centrifugation (30 min) using a bench Eppendorf centrifuge 5410 (Eppendorf-Netheler-Hinz, Hamburg, Germany), the supernatant was removed. The pellet was washed several times with diethyl ether and then lyophilized to obtain a dry powder.

NMR spectroscopy

SS-NMR spectroscopy was carried out using a Varian Inova 300 NMR spectrometer (Varian, Palo Alto, Calif., USA) operating at 75.45 MHz for ^{13}C and a Doty magic angle spinning (MAS) probe (Doty Scientific, Columbia, S.C., USA) using a 5 mm rotor. ^{13}C spectra were acquired using cross-polarization (CP) MAS (Andrew 1981) with a ^{1}H $\pi/2$ pulse of 3.6 μs, a contact time of 3 ms, a recycle delay of 2 s, a sweep width of 30 kHz and 8000 transients, and processed with a line broadening of 50 Hz. CP is used to enhance the ^{13}C signal by polarization transfer from protons to carbon (Pines et al. 1972; Homans 1992) and MAS to reduce the dipolar coupling and chemical shift anisotropy to obtain a well-resolved carbon spectrum.

Distance measurements

RR experiments were carried out by selectively inverting the ^{13}C-labelled carbonyl resonances of melittin using a soft π pulse and observing the subsequent exchange of magnetization between labelled resonances ([1-^{13}C]Leu13 melittin, [3-^{13}C]Phe4 inhibitor) while performing MAS at a spin rate satisfying the condition $\Delta\nu = n\nu_r$, where $\Delta\nu$ is the frequency separation between two labelled resonances, n is an integer and ν_r is the sample spinning speed (for a review, see Peersen and Smith 1993). A range of mixing times, τ_m, is employed to follow the magnetization transfer. As τ_m is increased, greater magnetization transfer between the two labelled carbons occurs, and the signal intensity of each resonance decreases. Analysis requires that spectra from samples containing native (natural abundance) peptides under identical conditions be subtracted to remove the background signal. Differences in peak intensity $< I_z - S_z >$, normalized to 1 at zero mixing time, are then plotted against τ_m to generate a magnetization exchange curve (Peersen and Smith 1993; Peersen et al. 1995). Chemical shifts were referenced to hexamethylbenzene (HMB).

Molecular modelling

Molecular modelling was used to interpret the NMR data obtained from a lyophilized powder of melittin-inhibitor complex. In an analogous fashion to our previous work (Lam et al. 2001), the structure of melittin in the melittin-inhibitor complex was modelled using DYANA (Güntert et al. 1997). Briefly, the crystal structure of melittin (Terwilliger and Eisenberg 1982) was used to derive a set of constraints to restrict the overall melittin conformation to a fold similar to that of the curved helix found in the crystal and solution structures. Additional constraints were included from measurements made using RR of distances around the Pro14 residue in melittin when bound to the inhibitor, e.g. [1-C]Leu13-[2-C]Leu16, [1-C]Leu13-[2-C]Ala15 and [2-C]Leu13-[1-C]Ala15, which showed no RR signal, were set to a lower distance limit of 6.5 Å. A relative weighting of 10 was used for the RR distances in the DYANA constraints to bias the final structures towards these values. Fifty structures were determined as described in Lam et al. (2001) and the best 20 analysed using MOLMOL (Koradi et al. 1996).

The structure of the melittin-inhibitor complex was also modelled using DYANA by incorporating the intermolecular distance found by RR between Phe4 of the inhibitor and Leu13 of melittin. Additional constraints derived from the signal decays observed in the Dy^{3+} SS-NMR analysis were also incorporated. Again, 50 structures were calculated using DYANA and the best 20 analysed.

Results and discussion

In order to locate the inhibitor binding sites in melittin, lanthanide ions were first bound to the inhibitor and the effect on the NMR spectra of labelled melittin examined. From the decrease in signal intensity of the labelled resonances in the presence of Dy^{3+}, appropriate residues were selected in melittin and the inhibitor for measurement of intermolecular distances by RR techniques.

Inhibitor-Dy^{3+}

Ac-IVIFDC-NH_2 is highly hydrophobic, with the single charged COO^- group on the aspartic acid being the most likely binding site for Dy^{3+} ions. The decay of signal intensities with titration of Dy^{3+} ions for the various carbon sites in the peptide correlates to the distance from the bound cation. Addition of Dy^{3+} lanthanide ions (0–4 mM) to the inhibitor resulted in a gradual loss of spectral intensity of Phe ring and backbone ^{13}C NMR resonances, with small chemical shift changes (Fig. 1a–c).

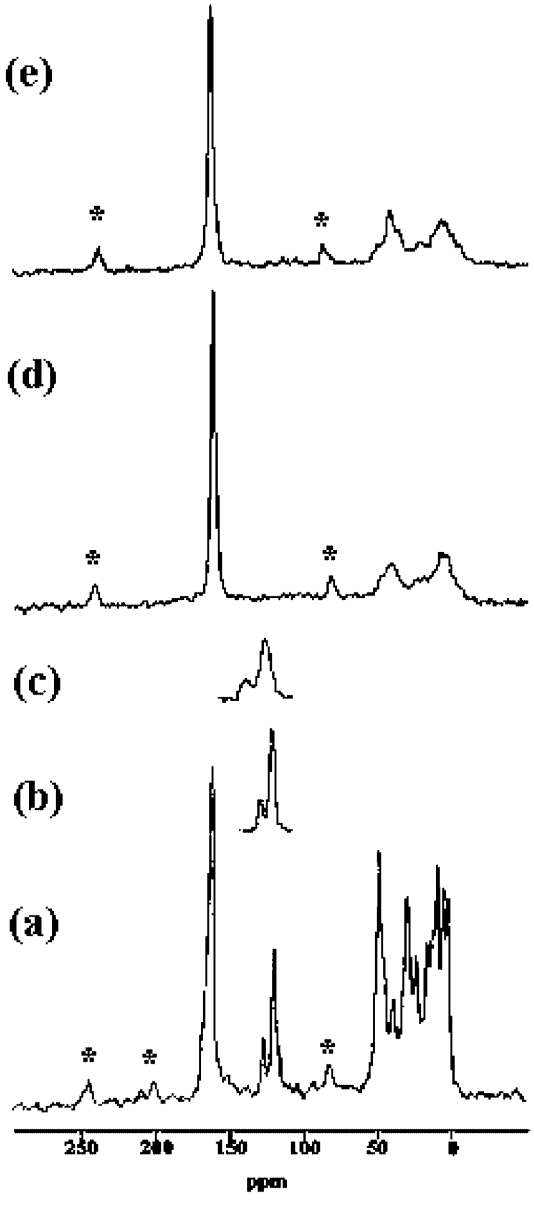

Fig. 1. ^{13}C CP MAS NMR spectra of melittin and inhibitor at room temperature using 6000 Hz spinning speed, 3 ms contact time, 1 s recycle delay and 4096 transients: **a** inhibitor alone, **b** inhibitor with 1 mM $DyCl_3$ (0.6 μmol), **c** inhibitor with 4 mM $DyCl_3$ (2.5 μmol), **d** [1-^{13}C]Ile17 melittin alone and **e** [1-^{13}C]Ile17 melittin with 1 mM $DyCl_3$ (0.5 μmol). Asterisks indicate MAS sidebands

This suggests that paramagnetic relaxation effect contributions to T_2 are larger than the chemical shift contribution, as observed for studies of lanthanide effects on small sonicated vesicles (Hauser et al. 1975) and bicelles (Prosser et al. 1998). An intensity decrease was observed for the aromatic ring of Phe (119 ppm), whereas no significant change in signal intensities was observed at the carbonyl and C_α, C_β and C_γ resonances of the inhibitor, suggesting that the lanthanide ion is bound to the side chain of an adjacent residue. No significant quenching of isoleucine resonances or the CH_3 resonance of Val2 was observed. This indicates that the binding site of the lanthanide ion is most likely the COO^- group of the aspartic acid, Asp5.

Melittin-Dy^{3+}

[1-^{13}C] specifically labelled melittin analogues (Ile2, Ala4, Val5, Leu6, Val8, Leu9, Leu13, Ala15, Ile17 and Ile20) complexed with Dy^{3+} showed no significant changes in signal intensity for labelled C-13 residues compared to melittin alone. For example, ^{13}C CP MAS spectra of [1-^{13}C]Ile17 melittin with and without Dy^{3+} are shown in Fig. 1d and Fig. 1e. The similarity of the spectra suggests that the Dy^{3+} was not bound to the melittin and is most likely related to the absence of potential binding sites (Asp or Glu) in the peptide sequence. Combined with our data showing that Dy^{3+} bound to the inhibitor only at Asp5, this allowed us to further explore the binding sites within the highly insoluble melittin-inhibitor complex.

Melittin-inhibitor complex

^{13}C CP MAS experiments were carried out using specifically labelled [1-^{13}C]Leu6-[^{15}N]Val8 melittin, [1-^{13}C]Leu13-[2-^{13}C]Leu16 melittin and [1-^{13}C]Ile17 melittin with inhibitor in a 2:3 mole ratio. No significant signal intensity changes in [1-^{13}C]Leu6 and [^{15}N]Val8 were observed as the concentration of the added Dy^{3+} solution increased from 0 to 4 mM, although a change in chemical shift was observed from 169 to 166.6 ppm for [1-^{13}C]Leu6. This suggested that this labelled site in melittin was not close to Asp5 of the inhibitor.

A significant change in relative intensity was observed in [1-^{13}C]Leu13-[2-^{13}C]Leu16 (Fig. 2) and [1-^{13}C]Ile17 with inhibitor Dy^{3+}. The relative intensity decay with 4 mM Dy^{3+} for the label of Leu13, Leu16 and Ile17 was ~50%, ~40% and ~20%, respectively. This result suggests that Leu13 of melittin is closer to Asp5 of the inhibitor than Ile17.

The above results support the model of Hewish et al. (1996) that the strongly hydrophobic inhibitor is expected to interact with the hydrophobic side of the amphiphilic melittin helix. Tryptophan or another aromatic at position 19 is known to be crucial for the lytic activity of melittin (Habermann and Kowallek 1970; Blondelle and Houghten 1991; Blondelle et al. 1993) and

it was proposed that the inhibitor masks this residue. Hewish et al. (1996) also suggest that the inhibitor lies adjacent to the hydrophobic area of melittin defined by the residues Val8, Leu9, Leu13, Leu16 and Ile20. However, our results suggest that Asp5 of the inhibitor was not near Val8, but rather closer to Leu13, Leu16 and Ile17.

The decay in signal intensity allows us to assess the proximity of the lanthanide ion. The decay in intensity of a labelled site gives an indication of the distance (with a r^{-6} distance dependence) to the Dy^{3+} binding site. A correlation between the relative distance within the melittin-inhibitor complex and the decay of relevant intensities was inferred. From the Dy^{3+} studies of the melittin-inhibitor complex, labelled sites were chosen in both the melittin and inhibitor for intermolecular distance measurements by RR.

Intermolecular distance measurements

The intermolecular distance measurements of the melittin-inhibitor complex were carried out using powder samples of [1-^{13}C]Leu13-[2-^{13}C]Leu16 melittin and [3-^{13}C]Phe4 inhibitor. The frequency in Hz between the chemical shift of the [2-^{13}C]Leu16 melittin and [3-^{13}C]Phe4 inhibitor were close (~2000 Hz) and a stable spinning speed, which is essential for the RR condition (Peersen and Smith 1993; Peersen et al. 1995), was difficult to sustain. The intermolecular distance between [1-^{13}C]Leu13 melittin and [3-^{13}C]Phe4 inhibitor was determined to be 3.8 ± 0.2 Å by RR (dipolar coupling of 140 Hz) (Fig. 3). From this result and the percentage decrease in signal intensity with Dy^{3+} of [2-^{13}C]Leu16, [1-^{13}C]Leu13 and [1-^{13}C]Ile17, it appears that the intermolecular distance of [2-^{13}C]Leu16 is closer than 3.8 Å and [1-^{13}C]Ile17 is greater than 3.8 Å. The intramolecular distances [1-^{13}C]Leu13-[2-^{13}C]Leu16 and [1-^{13}C]Leu13-[2-^{13}C]Ala15 in melittin with inhibitor were > 6.5 Å (Lam et al. 2000). The distance change and CD results (Lam et al. 2000) indicated a loss of α-helicity, possibly caused by strong binding between the inhibitor sidechain of Phe4 to the backbone of melittin around Pro14.

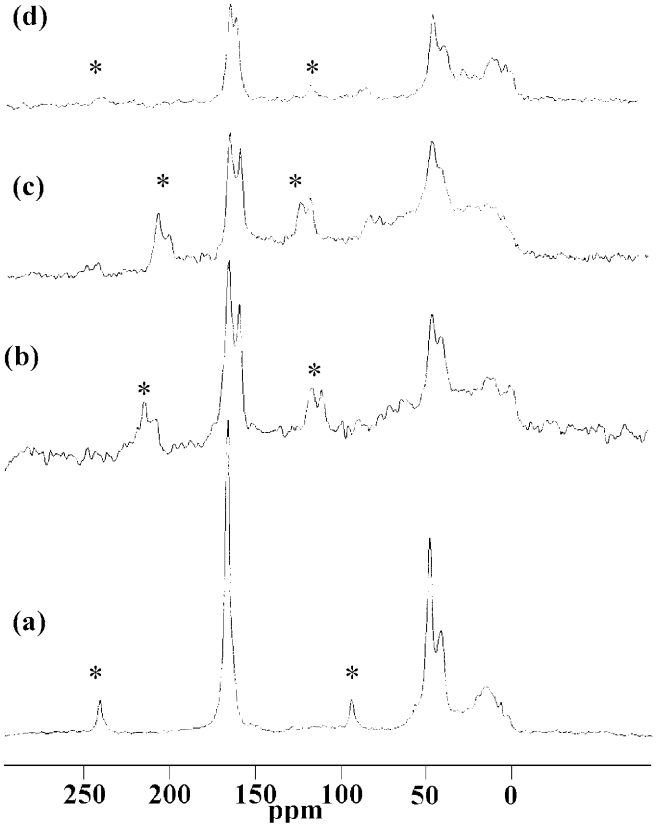

Fig. 2. **a** ^{13}C CP MAS NMR spectrum of labelled [1-^{13}C]Leu13-[2-^{13}C]Leu16 melittin-inhibitor complex, and with increasing concentrations of $DyCl_3$ solution: **b** 1 mM (0.5 μmol), **c** 2 mM (1 μmol) and **d** 4 mM (2 μmol). Asterisks indicate MAS sidebands

Molecular modelling of melittin-inhibitor complex

Molecular modelling was undertaken in order to interpret the observed intra- and intermolecular RR distances in the melittin-inhibitor complex. Modelling also allowed comparison of possible structural changes between melittin alone and when complexed to the inhibitor. The experimental intramolecular distances measured by RR for [1-^{13}C]Leu13-[2-^{13}C]Leu16 and [1-^{13}C]Leu13-[2-^{13}C]Ala15 melittin complexed with inhibitor were in excess of 6.5 Å, indicating a change in structure of the melittin (Lam et al. 2001). The melittin [1-^{13}C]Leu13 to inhibitor [3-^{13}C]Phe4 distance was found, by RR, to be 3.8 Å. Decay effects (Gröbner et al. 1999) observed for the melittin [1-^{13}C]Leu13, [2-^{13}C]Leu16 and [1-^{13}C]Ile17 resonances in the presence of Dy^{3+} and inhibitor indicated that Leu13 and Leu16 were approximately 3.8 Å from the Dy^{3+} ion where it is bound to the inhibitor,

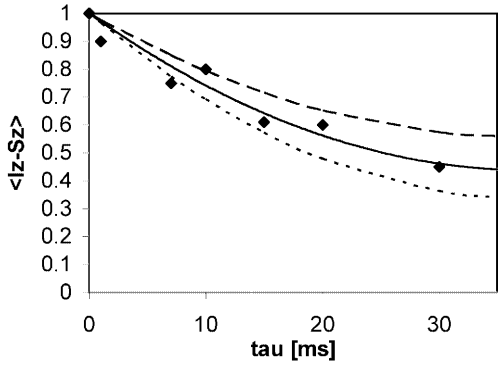

Fig. 3. The magnetization exchange curve for [1-^{13}C]Leu13 melittin to [3-^{13}C]Phe4 inhibitor as a dry powder determined from the RR spectra. The *symbols* on the graph are the data points obtained from experiment and the curve (*solid line*) was obtained by non-linear least-squares fitting of T_{2ZQ} and the dipolar coupling. The *dotted* and *dashed lines* are the simulation curves for the upper and lower distance limits

while Ile17 is further away, around 4.3 Å. Analysis of the structures of the melittin-inhibitor complex, calculated in DYANA and incorporating constraints derived from the RR data and SS-NMR using Dy^{3+}, indicates that two distinct orientations for the inhibitor are identified (Fig. 4). These differ in the positioning of the Phe4 sidechain of the inhibitor to one or other side of the melittin helix adjacent to Leu13 (Fig. 4A), with consequent adaptation of the rest of the inhibitor to satisfy the other constraints imposed during the calculation. The limited number of constraints currently available to pin down the inhibitor are insufficient to distinguish which of these two potential orientations actually occur; it is possible that both species are, in fact, present in the complex. The alteration of the structure of melittin is very similar in both conformations, with the most obvious effect being a straightening of the bend at Pro14 (see below). The majority of interactions between the inhibitor and melittin are towards the C-terminal end of melittin, with no interactions occurring with N-terminal residues of Pro14.

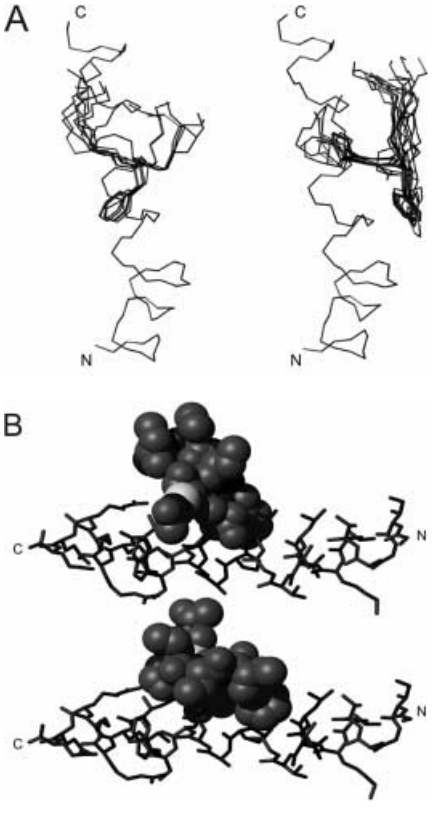

Fig. 4. **A** Diagrammatic representation of the two different melittin-inhibitor complex models derived from RR and Dy^{3+} quenching effects. In both cases a single representative melittin backbone trace is shown, with the N-terminus of the peptide at the bottom of the figure. All of the inhibitor structures from each family of structures are shown, with the sidechain of Phe4 only visible for clarity. In this view it is immediately apparent that the Phe4 sidechain of the inhibitor sits on one or other side of the melittin in the two groups of structures. This alters the orientation of the rest of the inhibitor to accommodate other constraints on the complex structure. **B** Diagrammatic representation of the lowest energy structures from each of the two families of melittin-inhibitor models. Melittin is shown as a *heavy-atom stick model*. The inhibitor is shown as a *CPK representation* and clearly interacts preferentially with C-terminal residues of the proline in both structures. Trp19 in melittin is indicated in both structures by the *dotted loop* and has been shown by both CD and fluorescence studies to be influenced by inhibitor binding

The inter-helical angles determined for melittin in the complex were compared with those from other results. The angles were measured at the intersection of two lines drawn through the axes of the helices defined by residues 1–13 and 17–26 (Lam et al. 2001). The angles measured between the N- and C- terminal α helices in the structures modelled for melittin bound to inhibitor fall in the range $176 \pm 5°$, which is greater than the angle of 129° obtained for the crystal structure (Terwilliger and Eisenberg 1982). Angles of $126 \pm 15°$ in dodecylphosphocholine (DPC) micelles (Inagaki et al. 1989) and $130 \pm 9°$ in lipid (Lam et al. 2001) have been reported. However, in aligned lipid bilayers in the fluid phase (Smith et al. 1994), an angle close to the 160° observed for melittin in methanol (Bazzo et al. 1988) was reported. While binding of the inhibitor resulted in a reduction in melittin α-helicity as determined by CD spectroscopy (Lam et al. 2000), the model structure of the complex does not show any marked degree of change in α-helicity. This is probably due to the method used to calculate the structure, with constraints derived from the crystal structure encouraging the formation of a helix by melittin. Determination of additional experimental constraints for the melittin-inhibitor complex and recalculation of the structure should clarify the extent of changes in helical content.

Figure 4B shows the two models of the melittin-inhibitor complex derived from our data, with melittin shown as a stick model and the inhibitor as CPK spheres. It is clear that, in both models, the inhibitor interacts almost exclusively with residues between Leu13 and Trp19 of the melittin. Our solution NMR studies of inhibitor titrated against melittin (Lam et al. 2000) demonstrate a change in chemical shift of the Trp19 sidechain resonance, in agreement with fluorescence studies by Hewish and coworkers (1996). Both models show close contacts between parts of the inhibitor and Trp19.

The above results suggest a mechanism for inhibition of melittin by the hexapeptide. The inhibitor is bound near the C-terminus of melittin, where it may mask the positively charged residues and reduce lipid-headgroup interactions. In addition, binding of the inhibitor appears to cause a change in the bend angle of melittin at Pro14 and a reduction in helicity, which would adversely affect solubility as reflected by precipitation of the melittin-inhibitor complex from solution. Further studies of the complex to determine additional structural constraints, as well as studies of the complex in membrane environments, are required to fully elucidate the mechanism of inhbition. Double-echo rotational resonance (REDOR) (Gullion 1998) techniques to measure heteronuclear distances up to 13 Å, e.g. ^{19}F Phe inhibitor-^{13}C melittin, are proposed.

Conclusions

Examination of melittin-inhibitor binding sites using lanthanide ions aided conformational studies of the complex. SS-NMR rotational resonance techniques (Peersen et al. 1993; Peersen et al. 1995) were used to measure inter- and intramolecular distances within the melittin-inhibitor complex.

In summary, strong binding between the lanthanide and the charged group of Asp5 in the inhibitor enabled an assessment of the binding sites between melittin and inhibitor. The relative intensity decay and chemical shift changes of labelled groups with increasing concentration of lanthanide ion suggested which residues in melittin were closely bound to the inhibitor. The results indicated that inhibitor was strongly bound around the Pro14–Trp19 region, in agreement with fluorescence studies (Hewish et al. 1996), but not near the N-terminus of melittin. The activity of melittin is dependent on Trp19 or an aromatic group at residue 19 (Dempsey 1990; Hewish et al. 1996), and the inhibitor may cause loss of biological activity by binding in this region.

The distance determined using RR between [1-^{13}C]Leu13 melittin-[3-^{13}C]Phe4 inhibitor came to 3.8 Å, indicating a close arrangement of melittin and inhibitor. CD data (Lam et al. 2000) show a loss of α-helicity when the inhibitor binds to melittin. The loss of cytolyic activity of melittin upon inhibitor binding may be due to a combination of conformational changes and masking of the aromatic sidechain, which prevents insertion of melittin into the lipid membrane.

References

Andrew ER (1981) Magic angle spinning in solid state NMR spectroscopy. Phil Trans R Soc Lond A 299:505–520

Bazzo R, Tappin MJ, Pastore A, Harvey TS, Carver JA, Campbell ID (1988) The structure of melittin. A ^{1}H-NMR study in methanol. Eur J Biochem 173:139–146

Blondelle SE, Houghten RA (1991) Probing the relationships between the structure and haemolytic activity of melittin with a complete set of leucine substitution analogs. Pept Res 4:12–18

Blondelle SE, Simpkins LR, Houghten RA (1993) In: Schneider CH, Eberle AN (eds) Peptides 1992. ESCOM, Amsterdam, pp 761–762

Dempsey CE (1990) The actions of melittin on membranes. Biochim Biophys Acta 1031:143–161

Gröbner G, Glaubitz C, Watts A (1999) Probing membrane surfaces and the location of membrane-embedded peptides by ^{13}C MAS NMR using lanthanide ions. J Magn Reson 141: 335–339

Gullion T (1998) Introduction to rotational-echo, double-resonance NMR. Concepts Magn Reson 10:277–289

Guntert P, Mumenthaler C, Wüthrich K (1997) Torsion angle dynamics for NMR structure calculations with the new program DYANA. J Mol Biol 273:283–298

Habermann E, Kowallek H (1970) Modifications of the amino groups and the tryptophan (residues) in melittin as a means of studying the relation between structure and mode of action. Hoppe-Seyler's Z Physiol Chem 351:884–890

Hauser H, Phillips MC, Levine BA, Williams RJB (1975) Ion-binding to phospholipids. Interaction of calcium and lanthanide ions with phosphatidylcholine (lecithin). Eur J Biochem 58:133–144

Henry GD, Sykes BD (1994) Methods to study membrane protein structure in solution. Methods Enzymol 239:515–535

Hewish D, Werkmeister J, Kirkpatrick A, Curtain C, Pantela G, Rivett DE (1996) Peptide inhibitors of melittin action. J Protein Chem 15:395–403

Homans SW (1992) A dictionary of concepts in NMR. Clarendon Press, Oxford

Inagaki F, Shimada K, Kawaguchi K, Hirano M, Terasawa I, Ikura T, Go N (1989) Structure of melittin bound to perdeuterated dodecylphosphocholine micelles as studied by two-dimensional NMR and distance geometry calculations. Biochemistry 28:5985–5991

Koradi R, Billeter M, Wüthrich K (1996) MOLMOL: a program for display and analysis of macromolecular structures. J Mol Graphics 14:51–55

Lam Y-H, Nguyen V, Fakaris E, Separovic F (2000) Conformation of melittin-inhibitor complex. J Protein Chem 19:529–534

Lam Y-H, Wassall SR, Morton CJ, Smith R, Separovic F (2001) Solid-state NMR structure determination of melittin in a lipid environment. Biophys J 81:2752–2761

Merrifield RB (1963) Solid-phase peptide synthesis. I. The synthesis of a tetrapeptide. J Am Chem Soc 85:2149–2151

Novabiochem (1999) Catalog & peptide synthesis handbook. Novabiochem, Laufelfingen, Switzerland, pp S1–S93

Peersen OB, Smith SO (1993) Solid-state NMR approaches for studying membrane protein structure. Concepts Magn Reson 5:303–317

Peersen OB, Groesbeek M, Aimoto S, Smith SO (1995) Analysis of rotational resonance magnetization exchange curves from crystalline peptides. J Am Chem Soc 117:7228–7237

Pines A, Gibby MG, Waugh JS (1972) Proton-enhanced nuclear induction spectroscopy. ^{13}C chemical shielding anisotropy in some organic solids. Chem Phys Lett 15:373–376

Prosser RS, Hwang JS, Vold RR (1998) Magnetically aligned phospholipid bilayers with positive ordering: a new model membrane system. Biophys J 74:2405–2418

Rivett DE, Hewish D, Kirkpatrick A, Werkmeister J (1999) Inhibiton of membrane-active peptides by fatty acid-peptide hybrids. J Protein Chem 18:291–295

Smith R, Separovic F, Milne TJ, Whittaker A, Bennett FM, Cornell BA, Makriyannis A (1994) Structure and orientation of the pore-forming peptide, melittin, in lipid bilayers. J Mol Biol 241:456–466

Stewart J, Young J (1984) Solid phase peptide synthesis. Pierce Chemical, Rockford, Ill., USA

Terwilliger TC, Eisenberg D (1982) The structure of melittin. I. Structure determination and partial refinement. J Biol Chem 257:6010–6015

Villalain J (1996) Location of cholesterol in model membranes by magic-angle-sample-spinning. Eur J Biochem, 241:586–593

Werkmeister JA, Kirkpatrick A, McKenzie JA, Rivett DE (1993) The effect of sequence variations and structure on the cytolytic activity of melittin peptides. Biochim Biophys Acta 1157:50–54